

Implementation of Dynamic Bandwidth Re-allocation in Optical Interconnects using Microring Resonators

Chander Kochar, Avinash Kodi and Ahmed Louri
 Department of Electrical and Computer Engineering
 University of Arizona, Tucson, AZ - 85721, USA
 email: louri@ece.arizona.edu

Abstract

Dynamic bandwidth re-allocation (DBR) technique balances traffic by re-allocating bandwidth from under utilized links to over utilized links. This results in significant improvement in overall throughput and latency. In previous study, passive optical devices, namely arrayed waveguide gratings (AWGs) and couplers were used to implement DBR [2]. Although the performance was significantly improved, the design was cost prohibitive since it required n^2 number of lasers per board (where n is the number of transmitters per board). In this paper we propose the implementation of DBR using silicon on insulator (SOI) based microring resonators. We call this technique row-column switch implementation. The proposed active implementation reduces the number of required lasers by a factor of n without any degradation in performance. Analytical and simulation studies were conducted to compare the passive implementation of DBR with the proposed active approach. This comparison included area, power consumption, throughput, power loss (dB), power-delay product and area-delay product. Results show that the proposed active switch provides throughput and latency similar to the passive implementation of DBR while dramatically improving cost by a factor of n . There is a slight increase in power consumption (0.4% for the worst case traffic) using the active switch implementation.

1. Introduction

A direct consequence of the increasing bandwidth requirements for high performance computing systems (HPCS) is an increase in both size and complexity of the systems, which in turn results in increasing power consumption. The size and complexity of HPCS has reached a stage where power is now one of the defining performance parameters. Achieving the increasing bandwidth demand within

the latency-power constraint is now becoming a major challenge in the semi-conductor industry. On the other hand optics has for long been envisioned as an alternate medium of interconnection due to the large bandwidth availability (THz range). This enables optical technology to carry data rates in the range of tera bits per second (Tbps) at low latency and power [1]. Optics also enables exploitation of bandwidth re-allocation due to the ability of a single optical fiber/waveguide to transmit more than one wavelength. In case of hot-spot traffic, or non-uniform traffic, it is observed that while certain links and channels are over utilized others remain idle or under utilized. Application of dynamic bandwidth re-allocation (DBR) techniques allows for a more even distribution of load amongst the different links and channels thereby improving throughput and latency. DBR has previously been implemented in [2] using only passive optical components such as couplers and AWGs. Although it achieved the desired results in throughput and latency, there were two main drawbacks: (1) it was cost prohibitive in terms of the number of lasers required (the implementation scales as $O(n^2)$ where n is the number of transmitters per board), and (2) it made use of AWGs, which are generally bulky and can cause problems with integration.

The active row-column design proposed in this paper enables any-to-any routing (i.e any wavelength can be routed to any destination), while overcoming the above mentioned problems. The number of transmitters required for the active row-column switch scales as $O(n)$ and does not use AWGs. Silicon on insulator (SOI) based ring resonators are used as the basic building blocks. These ring resonators can be used to build 1×2 wavelength selective optical switches that are fast (~ 10 ns), small ($\sim 10\mu m$ diameter), consume very little power ($\sim 19\mu Watt$) [3, 4] and can be fabricated using standard CMOS technology.

Application of microring resonators for integrated photonic networks was first proposed by Marcatili [5] in 1969. Since then, proposed applications of microring resonators include filters [6, 7]; modulators [3, 8, 9]; optical switches

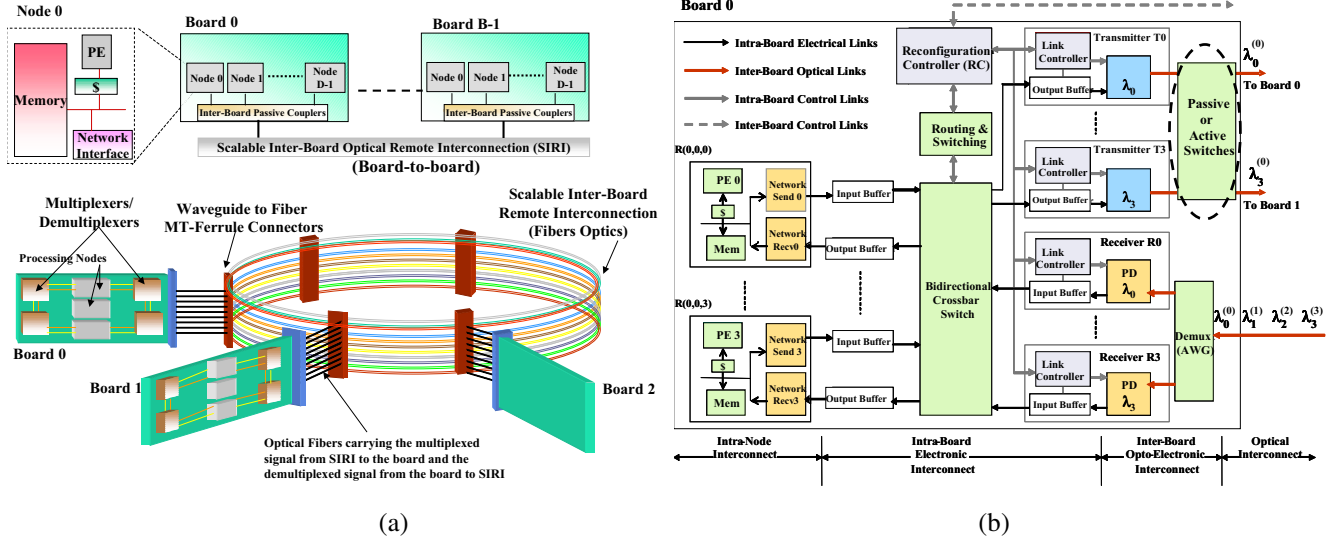


Figure 1. (a) E-RAPID architecture for C=1,B,D. (b) Interconnect design of E-RAPID Ref [2].

[4, 10, 11, 12]; optical crossconnects [13]; and lasers [14]. Despite the extensive research available in literature on ring resonators, it is only recently with advances in SOI technology that their application in photonic integrated circuits (PIC) has become feasible. There are two main advantages of using SOI microring resonators. (1) They can be fabricated using existing CMOS technology, allowing for a low cost solution to dense PIC and (2) High confinement of light allows for micrometer scale devices, which results in low area and power overheads.

2. DBR Implementation

2.1. E-RAPID Architecture

This section gives a brief introduction to E-RAPID [2] architecture and the routing and wavelength assignment (RWA) implemented for inter-board communication. E-RAPID network is defined as a 3-tuple (C, B, D) (Figure 1(a)), where C is the total number of clusters, B is the total number of boards per cluster, and D is the total number of nodes per board. As shown in Figure 1(b), the intra-board interconnect is an electronic bidirectional crossbar switch that routes packets between the nodes and the optical transmitters or receivers via the input and output buffers. The wavelength assigned from source board s to destination board d is given by $\lambda_{B-(d-s)}^{(s)}$ if $d > s$ and $\lambda_{(s-d)}^{(s)}$ if $s > d$, the superscript indicates the source board and the subscript indicates the wavelength to be transmitted on. However, due to the static scheme, only one wavelength is allocated between any pair of communicating boards irrespective of

the number of nodes on the board. This restriction can potentially lead to network congestion for non-uniform traffic patterns. DBR was proposed to overcome this limitation. For a complete description of the DBR algorithm please refer to [2].

2.2. DBR with Passive Components

Figure 2(a) shows how DBR may be implemented using an arrayed waveguide grating (AWG) for a (1,4,4) E-RAPID network [2]. Notice that there are now multiple laser sources per transmitter ($\lambda_0 - \lambda_3$). Each output buffer of a given transmitter is associated with 4 output ports (a, b, c and d). The notation $\lambda_x^{(y)}$ is used here to indicate wavelength x originating from port y for a given transmitter. As can be seen from the Figure 2(a) any wavelength can be used to transmit to any board. This allows re-allocation of load from an over utilized transmitter to an under utilized or idle transmitter. The downside of this approach is obvious, each transmitter requires lasers that cover the entire range of wavelengths. In other words, a board with n transmitters would require n^2 lasers.

2.3. DBR with Active Components

A microring resonator will couple light through it only if it satisfies the relation: $\lambda \times m = n_{eff} \times 2\pi R$, where R is the radius of the microring resonator, n_{eff} is the effective refractive index and m an integer. λ is then known as the resonant wavelength. By changing n_{eff} , the resonant wavelength of the microring resonator can be changed, enabling it to function as an optical switch [4], [10].

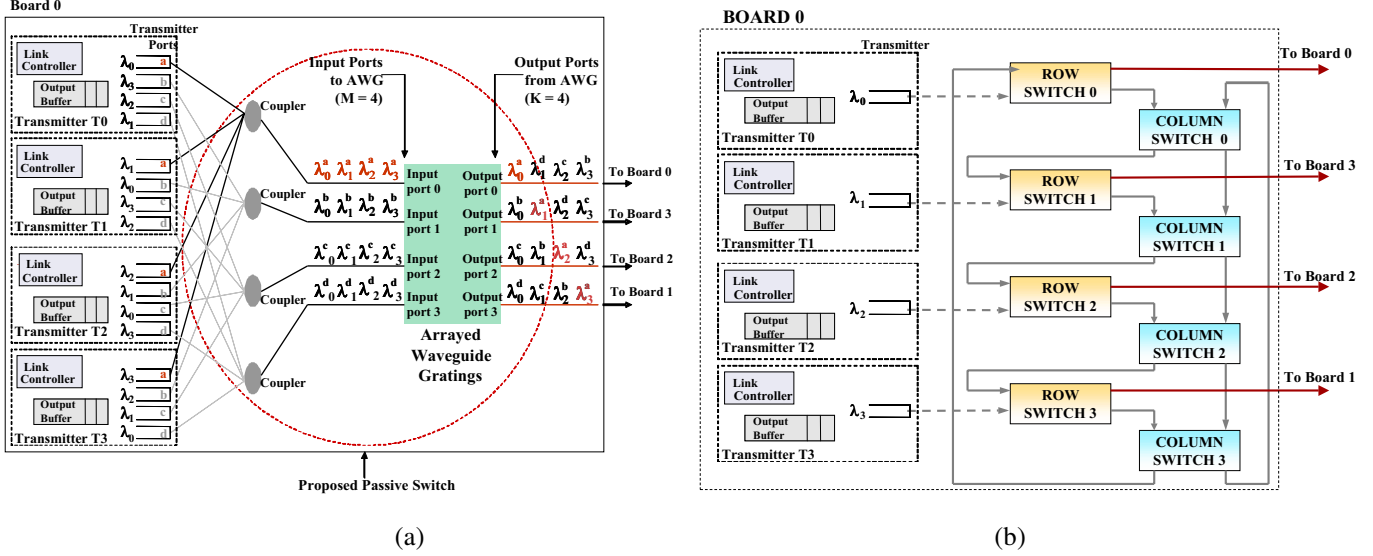


Figure 2. Implementation of DBR with (a) a passive switch. (b) an active switch.

The proposed switch consists of two dimensional row-column switches as shown in Figure 2(b). In contrast to the passive case, the number of lasers required is now n for a similar sized network (i.e. one laser per transmitter). The default or static output for transmitter k remains the same as described by the RWA [2]. In order to route transmitter k to some other output we make use of the column switches. The row and column switches are themselves 2×2 switches. The row switch k has the transmitter (shown by the dotted arrow) and the previous $k-1$ column switch as its input. Of the two outputs one is connected to the corresponding column switch (to re-direct the light to some other output), while the other output is the exit point from the switch matrix. The column switch has one of its inputs from the corresponding row switch as explained above and the second input is from the previous $k-1$ column switch. The outputs of the column switch are to the $k+1$ row (which will result in the signal exiting from the switch matrix at position $k+1$) and the next column switch (to further route the light to some other exit point). Due to the wavelength selective nature of the rings, light at each input can be individually routed to any output (although by default the input to a row switch from a previous column switch will always exit the switch matrix at that position). In general, for an $n \times n$ switch matrix we need n row switches and n column switches.

The detailed implementation of the proposed row-column switch is shown in Figure 3(a). As can be seen, a row switch requires only one ring resonator, which is resonant with the light from the corresponding transmitter (I_{R1}). Input from the previous column switch (I_{R0}) exits the

matrix by default at (O_{R0}). The two exit points of the row switch, (O_{R0}) results in an outlet to leave the switch matrix, where as (O_{R1}) sends the signal to the corresponding column switch. Of the two inputs to the column switch I_{C1} is the same as O_{R1} , while I_{C0} is the input from the previous column switch. There are n rings in the column switch which enable any input signal to be routed to any one of the two outputs independent of the other signals. Of the two output signals O_{C1} connects to I_{R0} of the next row switch where as O_{C0} connects to I_{C0} of the next column switch. By suitably controlling the applied voltages, V_{rw} (row voltage corresponding to wavelength w), and $V_{c0}, V_{c1}, \dots, V_{cw}, V_{cw+1}, \dots, V_{cN-1}$ (column voltages corresponding to the entire wavelength set, $\Lambda = \lambda_0, \lambda_1, \dots, \lambda_{N-1}$) to either V_{ON} or V_{OFF} , we can perform any-to-any switching (one-to-one, many-to-one, all-to-one) of all the wavelengths. Figure 3(a) also shows how to control the row and column switches to obtain the desired output. Since $V_{rw} = V_{ON}$ the wavelength does not exit from O_{R0} of row switch k , but instead is routed to O_{R1} . Light from O_{R1} is always directed towards the corresponding column switch, in this case column switch k . In the column switch, if $V_{cy} = V_{ON}$ (solid line) for a particular wavelength, the light does not couple to the ring resonator. As a result it goes to O_{C1} , which will result in it exiting the switch matrix from output $k+1$. On the other hand if $V_{cw} = V_{OFF}$ (dashed line), the light will go to O_{C0} and hence will proceed to the next column switch.

Another design consideration would be to use two rings per wavelength instead of one. Although this would increase area and optical power loss it has certain advantages. (1) Both the coupler and the u bend can be removed for

the row switch (as shown in Figure 3(b)). (2) The u bend from the column switch is no longer required. The above two points are possible because the switched light would now be traveling in the same direction as the input light. This offsets to some extent the increase in area due to the second ring. (3) Higher order filters provide better filtering characteristics with decreased adjacent channel cross talk [7]. Also, since only the lower ring requires to be turned on or off, there will be no extra penalty in terms of electrical power consumed if two rings are used instead of one.

2.4. Area and Cost Analysis

The area overhead of the ring resonator is calculated from [9] where, the radius is $5\mu m$, distance between ring and outer doping region is $0.5\mu m$, thickness of outer doping region is $3\mu m$ and width of trench (to provide sufficient isolation) is $2\mu m$. This results in an effective radius of $10.5\mu m$ for the ring resonator. For the u bend the inner radius was assumed to be $3\mu m$, since bending loss is negligible for any radius greater than $2\mu m$ [15]. As the coupler fits into an area of $25\mu m^2$ [16], for the sake of simplicity dimensions of the coupler were assumed to be $5\mu m \times 5\mu m$. On using two rings per switch instead of one, the width of the two ring system remains $21\mu m$. To calculate the total length care needs to be taken not to add the trench and outer doping thickness on the side where the two rings are coupled to one another. This gives the total length as $31.5\mu m$. Based upon the above values for an $n \times n$ switch matrix, the total area of 1 row switch + 1 column switch was calculated to be $(1770 + 630n)\mu m^2$ when using a single ring and $(1471.5 + 693n)\mu m^2$ when using a double ring. From [17], the area of a 4×4 SOI based AWG is $425 \times 155 \mu m^2$. Since there is no data available on higher radix SOI based AWGs, it was assumed that the area occupied by an AWG increases linearly with the radix (this is a reasonable assumption as it results in each dimension increasing by a factor of 1.4). The comparison of the area occupied by each method is shown in Figure 4, from which we can conclude that: (1) the area occupied by a double ring switch is not considerably more than that occupied by a single ring switch and (2) as the number of transmitters increases, the gap between passive and active switch areas decreases. This is primarily because we have assumed that an AWG scales linearly with size, where as the number of rings and hence the area occupied by the rings scales as $O(n^2)$. Table 1 shows a cost analysis of building an optical cross connect using passive and active technologies. From the table it is observed that even for a moderate value of n , the cost savings in terms of transmitters is significant. For example, in a 64 node E-RAPID system, while a passive switch would require 64 lasers per board, the active switch requires only 8, thus saving on 56 lasers per board or 448 lasers for the entire system.

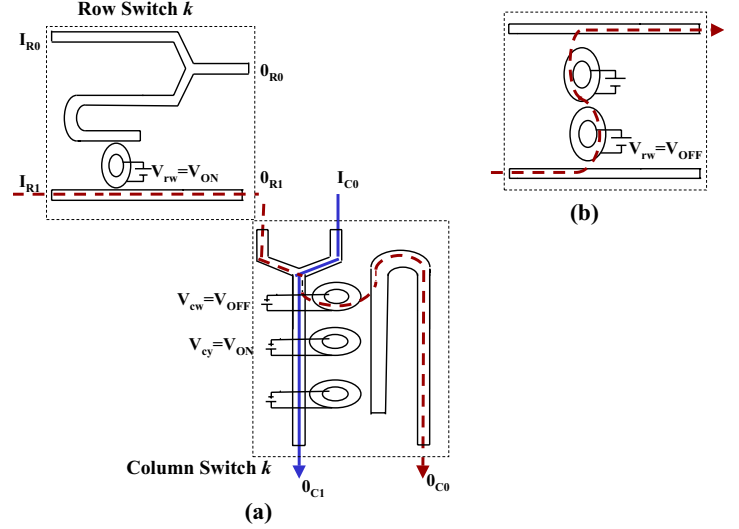


Figure 3. (a) Detailed implementation of row-column switch. V_{rw} and V_{cw} correspond to row and column voltages respectively for wavelength w . (b) Implementation of row switch using two rings.

3. Performance Evaluation

E-RAPID is evaluated using NETSIM and YACSIM (<http://www.ece.rice.edu/prrt.html>). Packets were injected according to Bernoulli process based on the network load for a given simulation run. The network load is varied from 0.1 – 0.9 of the network capacity. For the router model designed, the channel width is 16 bits and speed is 400 Mhz, resulting in a unidirectional bandwidth of 6.4 Gbps and per-port bidirectional bandwidth of 12.8 Gbps. Routing computation, virtual channel and switch allocation, each takes one router clock cycle. For the optical network, we assume bit rate of 5 Gbps. At 5 Gbps, the total power consumption of an optical link to transmit and receive a 64 byte packet, operating at a supply voltage of 0.9 V, is 43.03 mW [2].

The performance of E-RAPID was compared with active and passive switches for several communication patterns including uniform, butterfly, complement, perfect shuffle and matrix transpose for network size of 64 nodes. The performance of E-RAPID was compared on the basis of throughput, power consumed, power dissipation, area-delay product and power-delay product.

3.1 Throughput and Latency Results

Figure 5(a) and (b) show the effect of bandwidth re-allocation for complement and butterfly traffic patterns. Due to the nature of complement traffic all the nodes on

Table 1. Cost function per board for $n \times n$ E-RAPID System (assuming $C = 1$)SR stands for single ring, DR stands for double ring.

	Lasers	Couplers	AWG	Optical Sw	Area(μm^2)
Active(SR)	n	$2n$	0	$n(n+1)$	$n(1770 + 630n)$
Active(DR)	n	n	0	$2n(n+1)$	$n(1471.5 + 693n)$
Passive	n^2	$n(n-1)$	1	0	Area _{AWG} + $25n(n-1)$

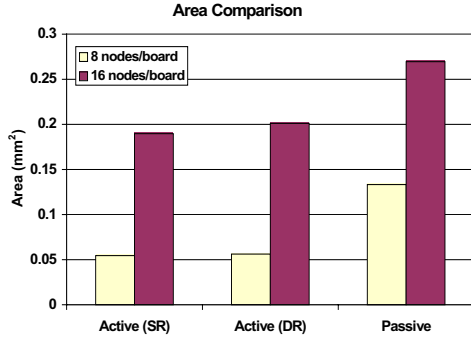


Figure 4. Area comparison for switch matrix using different design methodologies. SR - single ring, DR- double ring.

a board communicate with the same destination board. As a result, without bandwidth re-allocation only one transmitter is active per board resulting in high latency and low throughput. Therefore, re-allocation starts at very low loads and the system is fully reconfigured at a load of 0.2 (Figure 5(a)). For butterfly traffic, re-allocation occurs, but more slowly and to a lesser extent as compared to complement traffic and therefore reaches full reconfiguration at a load of 0.4. On attaining steady state, for complement reconfiguration improves throughput by over 400%, while throughput improvement for butterfly traffic is seen to be 25%. Both active and passive switch devices show similar performance with and without reconfiguration. In fact, complement ensures maximum possible reconfiguration in the system and thus shows the worst case power consumption and power loss for the active switch design. The affect on latency was negligible as the reconfiguration window (2000 cycles) is much larger than the switching time of a switch (4 cycles).

3.2. Power Consumption and Optical Power Budget

The total electrical power (P_T) consumed is calculated using the following formula, $P_T = \sum_{j=0}^B N_{Bj} \times P_{Tx/Rx} +$

$\sum_{j=0}^n N_{Rj} \times P_{ring}$, where B is the total number of boards, N_{Bj} is the total number of optical packets transmitted by Board j , $P_{Tx/Rx}$ is the electrical power to transmit and receive a single 64 byte optical packet, N_{Rj} is the number of times a switch in the on state is traversed by packets from board j , n is the size of the optical switch and P_{ring} is the electrical power consumed when a ring resonator is on. Theoretical calculations estimate the power consumption of a $5 \mu m$ radius microring resonator to be $19 \mu Watt$ [3]. Although current prototypes consume $1 mWatt$, straightforward fabrication advances can reduce this value to $100 \mu Watt$ [10]. Therefore we assume that each ring consumes $100 \mu Watt$, i.e. $P_{ring} = 100 \mu Watt$. Figure 5(c) shows the normalized electrical power consumption for the four traffic traces. As expected, for uniform and matrix transpose traffic patterns there is no extra power consumption since no reconfiguration occurs. Complement traffic results in maximum power consumption, which is about 0.41% more than the passive case. In complement traffic all switches are turned on for reconfiguration. Figure 5(d) shows the normalized average power dissipation per packet due to the four traffic traces. In all four cases, the power dissipation per packet is lower in the active case than the passive case. This is primarily due to the -3.5dB AWG loss for each packet in the passive case. It is worth noting that as reconfiguration takes place the average loss per packet for complement and butterfly increases until reconfiguration has reached a steady state. Figure 5(e) shows the power-delay product (PDP) for active and passive switch design for complement traffic. The PDP values of the two switch designs almost overlap because the power and latency penalty of using the active switch is minimal. Figure 5(f) shows the area-delay product (ADP) for complement traffic for a 64 node RAPID network. We see that as the load increases, the advantage of using an active switch design increases.

We next calculate the optical power budget. Figure 6 shows a simplified model from source to receiver and optical power losses associated in an E-RAPID system. The main components are lasers, waveguides/fibers, optical switches (which consists of row switches indicated by R and column switches indicated by C), directional couplers, demultiplexers and optical receivers. The following

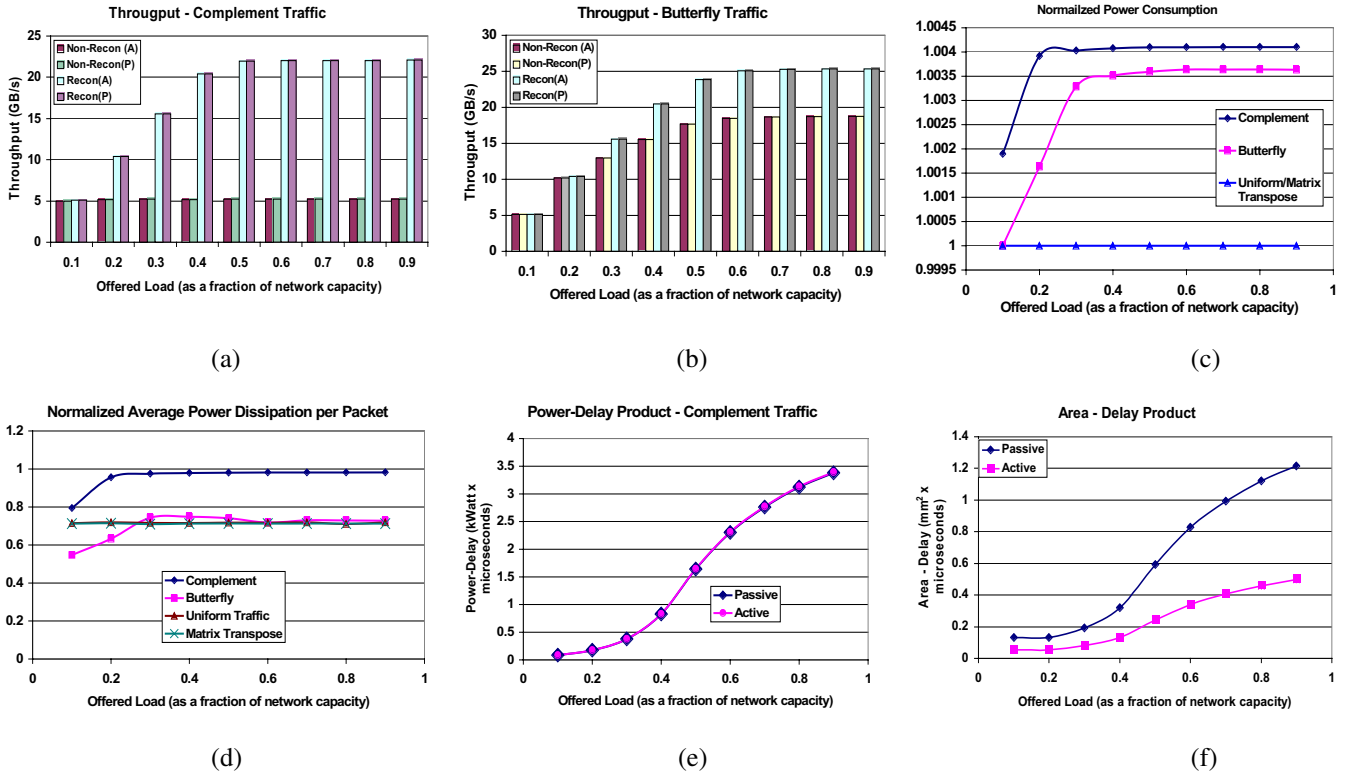


Figure 5. 64 node E-RAPID (a)-(b)Throughput comparison with active and passive switch design. (c)-(d) Normalized power values. (e)-(f)Power-Delay Product and Area-Delay Product with active and passive switch design.

losses exist in the system; source to waveguide coupling loss (L_{SW}), row switch loss (L_{RS}), column switch loss (L_{CS}), fiber to waveguide coupling loss ($L_{F/W}$), propagation loss in the fiber (L_F), waveguide to fiber coupling ($L_{W/F}$), directional coupler loss (L_{DC}), demultiplexer loss (L_D) and waveguide to receiver coupling loss (L_{WR}). Each row switch and column switch further consists of a ring resonator and an on-chip coupler. Thus L_{RS} and L_{CS} are themselves functions of ring resonator loss (L_{RR}) and on-chip coupler loss (L_C). It should also be noted that the losses in the row switch and column switch are different depending on whether the ring resonators are either turned on or off for each wavelength. If a row switch is on for a given wavelength, the loss (L_{RS_on}), is negligible as light only has to flow through a straight waveguide. On the other hand, if the row switch is off for a given wavelength, light couples through both the ring resonator as well as the on-chip coupler, therefore the loss (L_{RS_off}) is given by $L_{RS_off} = L_{RR} + L_C$. Similarly, if a column switch is on, there is only on-chip coupler loss and therefore $L_{CS_on} = L_C$. If a column switch is off, then the loss

is given by $L_{CS_off} = L_{RR} + L_C$ as the light will couple into both the on-chip coupler and the ring resonator.

When calculating the power budget, the worst case optical power loss (OPL) must be considered. For an $n \times n$ system (where n equals number of boards and the size of the optical switch) the worst case occurs when light has to go through $n - 1$ column switches before it leaves the board. This light will then have to couple with light from $n - 2$ other boards further adding to the loss. Therefore, the worst case $OPL = L_{SW} + L_{RS_on} + (n - 2) * L_{CS_off} + L_{CS_on} + L_C + L_{W/F} + L_F + (n - 1) * L_{DC} + L_{F/W} + L_D + L_{WR}$. For known optical power loss and receiver sensitivity of the system, the optical power required from the source may be determined from the equation $P_S - P_R \geq OPL$, where P_S is the source power in dBm, P_R is the minimum required receiver power also in dBm and OPL is in dB. P_R depends on the minimum bit error rate. For a BER of 10^{-15} , the received power P_R should be $-20dBm$ [18]. Assuming $L_{SW} = 1dB$, $L_C = 0.2dB$ [16], $L_{DC} = 0.5dB$ [19], $L_{RR} = L_D = 1dB$, $L_F = 1dB$, $L_{F/W} = 1dB$ and $L_{WR} = 0.5dB$, for the

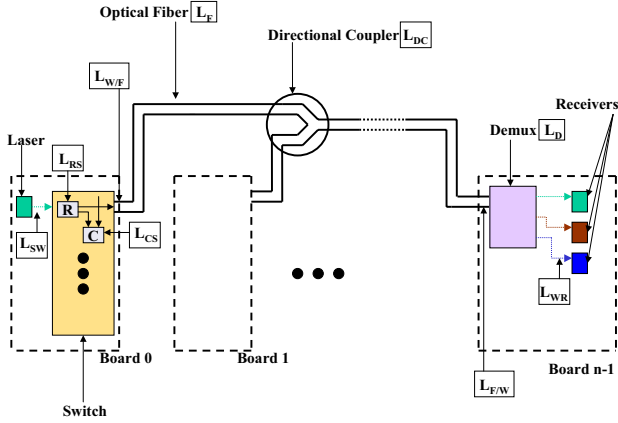


Figure 6. E-RAPID power model with components and associated optical losses.

single ring per switch, the worst case optical loss equals $OPL_{SR} = 4.9 + 1.2(n - 2) + 0.5(n - 1)$ dB. This can further be reduced to $OPL_{SR} = (1.7n + 2)$ dB. The worst case optical loss when using a double ring switch is given by $OPL_{DR} = 4.9 + 2.2(n - 2) + 0.5(n - 1)$ dB, which can be simplified to $OPL_{DR} = (2.7n)$ dB. Table 2 shows how the system can scale with increasing values of P_S from 2mW upto 40 mW. In the table P_S indicates source power, n_{SR} indicates the maximum number of boards possible using a single ring optical switch and n_{DR} indicates the maximum number of boards possible using a double ring optical switch. From Table 2 we see that as P_S increases, the maximum tolerable loss also increases but each increase is less than the previous one. This results in n_{SR} and n_{DR} not increasing linearly with increase in input power. With $P_S = 40mW$, the system can scale to 20 boards. Then assuming 20 nodes per board, a 400 node system may be built without need for amplification.

3.3. Effects of Frequency of Reconfiguration

Figure 7 shows how throughput, latency and power consumption vary as we change the amount of reconfiguration in a 64 node E-RAPID system with complement traffic and a load of 0.5. In the figure, $k = i$ implies i extra transmitters have been turned on. The load can now be evenly distributed between $i + 1$ different transmitters. From Figure 7(a) the throughput increases as the amount of reconfiguration increases. Average latency on the other hand decreases with reconfiguration (Figure 7(b)) due to the fact that a packet now undergoes lower blocking and queuing delays. To calculate total electrical power consumed, the formula for P_T derived in section 3.2 was used. Figure 7(c)

Table 2. Scaling of E-RAPID System with increasing source power (P_S) where n_{SR} and n_{DR} indicate the maximum number of boards possible using a single ring and a double ring optical switch respectively.

P_S (mW)	P_S (dBm)	n_{SR}	n_{DR}
2	3.0102	12	8
4	6.0205	14	9
6	7.7815	15	10
8	9.0302	16	10
10	10	16	11
20	13.0102	18	12
40	16.0205	20	14

shows more power is consumed by the active switch design when compared to the passive. In the worst case, the active switch consumes 0.41% more power when all the switches have been turned on.

4. Conclusion

In this paper a compact, integratable and non-blocking optical switch matrix for implementing dynamic bandwidth re-allocation is proposed. The switch matrix was designed to reduce cost (in terms of number of lasers) while maintaining the performance benefits and flexibility shown by passive implementation of DBR. SOI based ring resonators used as 1×2 optical switches were the basic building blocks of the proposed active row-column switch. Analytical and simulation studies show that the proposed active implementation provides throughput and latency similar to the passive implementation while dramatically improving cost by a factor of n (where n is the number of transmitters per board). There is a slight increase in power consumption (0.4% at most for the worst case traffic) using the active switch matrix.

5. Acknowledgment

This research was supported by NSF grants CCR-0309537 and CCF-0538945.

References

- [1] D. A. B. Miller, "Rationale and challenges for optical interconnects to electronic chips," *Proceedings Of IEEE*, vol. 8, no. 6, pp. 728–749, June 2000.

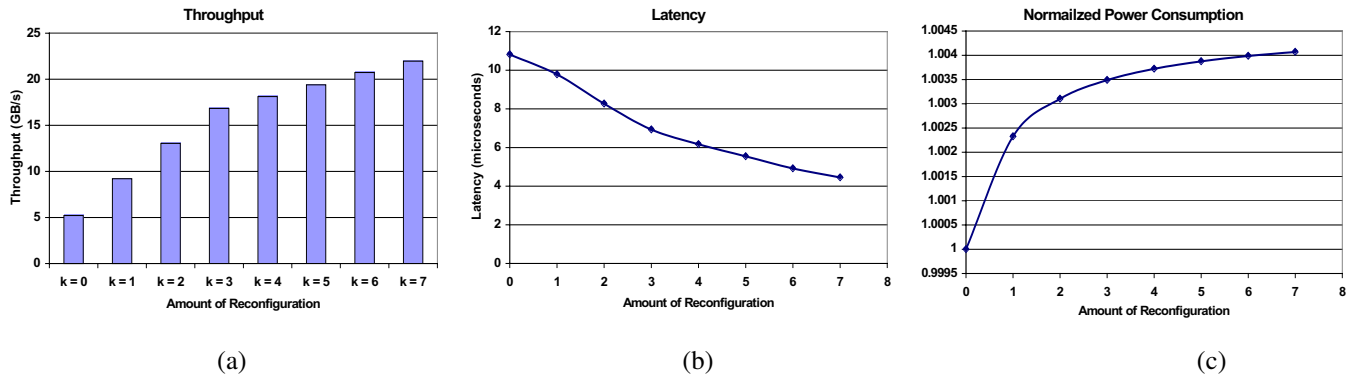


Figure 7. Variation in throughput, latency, normalized power consumption for a 64 node E-RAPID system under complement traffic and 0.5 load

- [2] A. K. Kodi and A. Louri, "Power-aware bandwidth-reconfigurable optical interconnects for high-performance computing (hpc) systems," in *21st IEEE International Parallel and Distributed Processing Symposium (IPDPS'07)*, Long Beach, California, March 2007.
- [3] Q. Xu, B. Schmidt, S. Pradhan, and M. Lipson, "Micrometre-scale silicon electro-optic modulator," *Nature Letters*, vol. 435, pp. 325–327, May 2005.
- [4] B. A. Lee, B. G. Small, K. Bergman, Q. Xu, and M. Lipson, "Transmission of high data rate optical signals through a micrometer-scale silicon ring resonator," *Optics Letters*, vol. 31, no. 18, pp. 2701–2703, September 2006.
- [5] E. A. J. Marcatili, "Bends in optical dielectric guides," *Bell Syst. Tech. J.*, vol. 48, pp. 2103–2132, 1969.
- [6] T. Barwicz, H. Byun, F. Gan, C. Holzwarth, M. Popovic, P. Rakich, M. Watts, E. Ippen, F. Kartner, H. Smith, J.S.Orcutt, R. Ram, V. Stojanovic, O. O. ana J.L. Hoyt, S. Spector, M. Geis, M. Grein, T. Lyszczarz, and J. Yoon, "Silicon photonics for compact energy-efficient interconnects," *Journal of Optical Networking*, vol. 6, no. 1, pp. 63–73, January 2007.
- [7] B.E.Little, S.T.Chu, H.A.Haus, J.Foresi, and J.P.Laine, "Microring resonator channel dropping filters," *Journal of Lightwave Technology*, vol. 15, no. 6, pp. 998–1005, June 1997.
- [8] V. R. Almedia, C. A. Barrios, R. R. Panepucci, and M. Lipson, "All optical control of light on a silicon chip," *Nature*, vol. 431, pp. 1081–1084, October 2004.
- [9] L. Zhou and A. W. Poon, "Silicon electro-optic modulators using p-i-n diodes embedded 10-micron diameter microdisk resonators," *Optics Express*, vol. 14, no. 15, pp. 6851–6857, July 2006.
- [10] B. A. Small, B. G. Lee, K. Bergman, Q. Xu, and M. Lipson, "Multiple-wavelength integrated photonic networks based on microring resonator devices," *Journal of Optical Networking*, vol. 6, no. 2, pp. 112–120, February 2007.
- [11] B. E. Little, H. A. Haus, J. S. Foresi, L. C. Kimerling, E. P. Ippen, and D. J. Ripin, "Wavelength switching and routing using absorption and resonance," *IEEE Photonics Technology Letters*, vol. 10, no. 6, pp. 816–818, June 1998.
- [12] T. A. Ibrahim, W. Cao, Y. Kim, J. Li, J. Goldhar, P. T. Ho, and C. H. Lee, "All-optical switching in a laterally coupled microring resonator by carrier injection," *IEEE Photonics Technology Letters*, vol. 15, no. 1, pp. 36–38, January 2003.
- [13] R. A. Soref and B. E. Little, "Proposed n-wavelength m-fiber wdm crossconnect switch using active microring resonators," *IEEE Photonics Technology Letters*, vol. 10, no. 8, pp. 1121–1123, August 1998.
- [14] H. Rong, Y.-H. Kuo, S. Xu, A. Liu, R. Jones, and M. Paniccia, "Monolithic integrated raman silicon laser," *Optics Express*, vol. 14, pp. 6705–6712, July 2006.
- [15] I. O'Connor, "Optical solutions for system level interconnects," in *Proc. 2004 International Workshop on System Level Interconnect Prediction (SLIP'04)*, Paris, France, February 2004, pp. 290–294.
- [16] A. Sakai, T. Fukazawa, and T. Baba, "Low loss ultra small branches in a silicon photonic wire," *IEICE Trans. Electron.*, vol. E85-C, no. 4, pp. 79–88, April 2002.
- [17] P. Dumon, W. Bogaerts, D. V. Thourhout, D. Taillaert, and R. Baets, "Compact wavelength router based on a silicon-on-insulator arrayed waveguide grating pigtailed to a fiber array," *Optics Express*, vol. 14, no. 2, pp. 664–669, January 2006.
- [18] A. K. Kodi and A. Louri, "Rapid: Reconfigurable and scalable all-photonic interconnect for distributed shared memory multiprocessors," *Journal of Lightwave Technology*, vol. 22, no. 9, pp. 2101–2110, September 2004.
- [19] E.C.M.Pennings, R.J.Deri, A.Scherer, R.Bhat, T.R.Hayes, N.C.Andreadakis, M.K.Smit, L.B.Soldano, and R.J.Hawkins, "Ultra-compact, low-loss directional couplers on inp based on self-imaging by multimode interference," *Applied Physics Letters*, vol. 59, no. 16, pp. 1926–1928, October 1991.